Photonic crystal optical waveguides for on-chip Bose-Einstein condensates

J. Bravo-Abad,* M. Ibanescu, J. D. Joannopoulos, and M. Soljačić
Center for Materials Science and Engineering and Department of Physics, MIT, Cambridge, Massachusetts 02139, USA
(Received 3 June 2006; published 20 November 2006)

We propose an on-chip optical waveguide for Bose-Einstein condensates based on the evanescent light fields created by surface states of a photonic crystal. It is shown that the modal properties of these surface states can be tailored to confine the condensate at distances from the chip surface significantly longer that those that can be reached by using conventional index-contrast guidance. We numerically demonstrate that by index-guiding the surface states through two parallel waveguides, the atomic cloud can be confined in a two-dimensional trap at about 1 μm above the structure using a power of 0.1 mW.

DOI: 10.1103/PhysRevA.74.053619 PACS number(s): 03.75.−b, 42.70.Qs, 42.82.Et

Magnetic microtraps able to guide Bose-Einstein condensates (BECs) have been proposed as a promising way to implement on-chip matter-wave waveguides [1]. However, this technology is restricted by a fundamental limitation: the trapping mechanism works for only a subset of hyperfine states for any given trapping magnetic field. It has been shown that this limitation can be circumvented in a purely optical trap, where atoms in all hyperfine states can be confined [2]. When working with an optical trap, one has the possibility of modifying the atomic interaction of a BEC by simply varying the external magnetic field [3]. This could be of paramount importance for the development of efficient Sagnac interferometers based on two counterpropagating matter waves. Due to the mentioned interest, different kinds of dielectric structures have been proposed as optical traps [4–13]. However, the extension of these ideas to create optical on-chip BEC waveguides and circuits is limited.

One of the simplest schemes one could imagine for on-chip waveguiding of BECs would be to use the evanescent electric field produced by illuminating a high-index waveguide (ϵ_{wav}) deposited on top of a uniform dielectric substrate of dielectric constant ϵ_{subs} (with $\epsilon_{wav} > \epsilon_{subs}$). In order to have index guiding in the waveguide, without leakage into the substrate, the wave vector k of the guided mode has to satisfy $k > (\omega/c)\sqrt{\epsilon_{subs}}$. This in turn means that the decay constant of the evanescent tails into air is given by $\alpha = \sqrt{k^2 - \omega^2/c^2} > (2\pi/\lambda_{air})\sqrt{\epsilon_{subs}-1}$, where λ_{air} is the wavelength of light in air. Because ϵ_{subs} cannot be close to unity (it is typically larger than 2.0), this is a fast decay that would prevent the balance between the repulsion from the surface and the Casimir-Polder attraction. For similar reasons, the same constraints apply for any index-guided scheme that involves a solid-state substrate for which $\epsilon_{subs} - 1 \sim 1$. On the other hand, designs without a substrate would have thickness below λ_{air}, rendering them very fragile and difficult to work with.

In this work, we move a step forward and we show that the use of a photonic crystal (PhC) as a substrate would permit decay lengths long enough to circumvent the limits imposed by the Casimir-Polder attraction. We introduce a design for optical waveguiding of BEC based on a class of surface state waveguides. In the proposed system, the surface states of a one-dimensional (1D) photonic crystal [15] are confined to propagate along a waveguide built into a defect of the PhC by means of a suitable combination of both photonic band gap and total internal reflection (TIR) effects. This kind of waveguiding mechanism is unique to PhCs.

Figure 1 shows a schematic picture of the structure analyzed in this work for on-chip BEC waveguiding. The main idea proposed here to get a confining potential both in the x and y directions (see the reference system in Fig. 1) is the following. First, we create a 1D PhC by a periodic sequence of high-dielectric-constant (ϵ_{hi}) and low-dielectric-constant (ϵ_{lo}) layers (plotted as red and yellow volumes in Fig. 1, respectively). The thickness of each layer is given by W_{hi} and W_{lo}. In addition, we define a as the periodicity of the PhC. Second, we introduce a defect in this structure by reducing the thickness of its top layer to W_d. The electric field of this defect mode is confined in both $y>0$ and $y<0$ regions, i.e., this mode is a surface state. By coupling into the defect layer a laser beam whose frequency is blue detuned from a certain transition of the atoms forming the considered BEC, the condensate will experience a repulsive potential from the surface. This potential combined with the Casimir-Polder interaction and the force exerted by gravity (which pushes the atoms toward the surface) will trap the BEC in the minimum of the potential in the y direction.

Once a suitable confinement in the direction normal to the air-PhC interface is obtained, the next step is to design a practical mechanism to confine the BEC in the x direction. We have found that one convenient way to achieve this is to create two index-guided parallel waveguides for these surfaces states (represented as blue volumes in Fig. 1, where W_w and H_w stand for the width of the waveguides and the separation between them, respectively). It is worth commenting that, to the best of our knowledge, it is the first time that such a waveguiding mechanism for PhC surface states has been proposed.

In order to optimize the potential created by the structure described in the previous paragraphs we first analyze the case in which the PhC is uniform in the x direction (i.e., without waveguides). This is a good starting point because

*Present address: Departamento de Física Teórica de la Materia Condensada, Universidad Autónoma de Madrid, E-28049 Madrid, Spain.

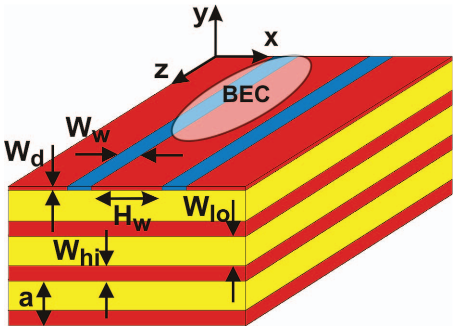

FIG. 1. (Color) Schematic picture of the structure proposed for BEC waveguiding. The system consists of a one-dimensional photonic crystal with a defect layer on its top. In the defect layer two parallel index-guiding waveguides are included. As sketched in the figure, for a suitable design of the system, the BEC cloud can be confined in the region between these waveguides. The reference system used throughout the text, together with the geometrical parameters defining the structure are also shown.

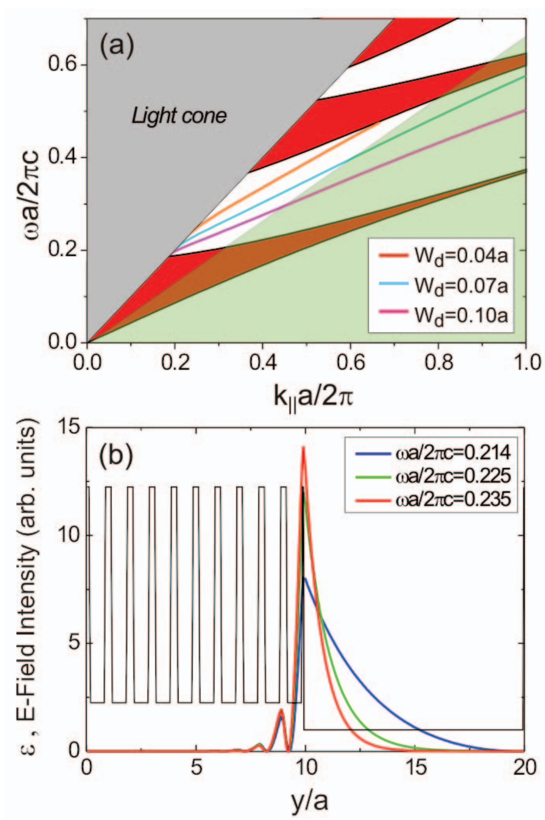

FIG. 2. (Color) (a) Projected band structure of the semi-infinite one-dimensional photonic crystal considered in this work [see the profile of dielectric constant in (b)]. Red-shaded areas show the regions where there exist extended states inside the PhC. Gray-shaded area corresponds to eigenmodes that are propagating in air. Orange, blue, and magenta lines represent the dispersion relations of the surface states for several values of the thickness of the top layer. Green-shaded region corresponds to possible confined states of any defect layer if it lies on top of a uniform dielectric substrate with $\epsilon=\epsilon_{lo}$. (b) Dielectric constant (black line) and electric field intensity profiles along the direction perpendicular to the interface PhC-air. Three surfaces states with frequencies close to the light line are displayed for $W_d=0.07a$.

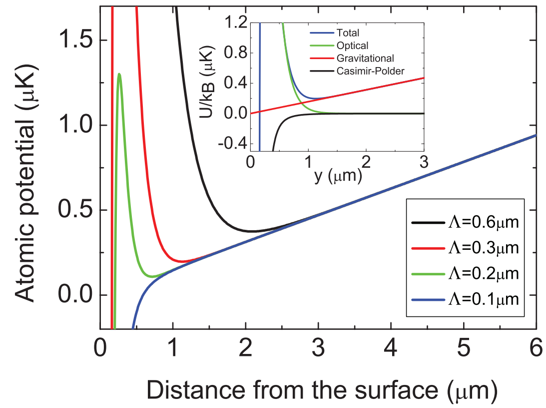

FIG. 3. (Color) Main panel: Total atomic potential for the case of Cs atoms as a function of the distance to the dielectric surface. The results for several decay lengths of the evanescent light field are shown. The optical dipole potential is assumed to be created by a Ti:sapphire laser at a wavelength of 839 nm. All the cases plotted in this figure were computed for the same intensity $I_0=2.67\times10^6$ mW/cm^2 evaluated just above the PhC-air interface. Inset: Total, optical, gravitational, and Casimir-Polder potentials (blue, green, red, and black, respectively) for the case of $\Lambda=0.3$ μm. The minimum for the total potential is found at $y_0=1.1$ μm.

the decay of the electric field in the y direction will be almost the same as in the system with the two waveguides [16].

Red regions in Fig. 2(a) show the projected bands of a semi-infinite 1D PhC computed by means of the plane-wave expansion method to Maxwell's equations [17]. Notice that in this figure $k_{\parallel}$ labels the wave vector along the PhC interface (i.e., $y=0$). We have taken the following values for the parameters defining the structure: $\epsilon_{hi}=12.25$, $\epsilon_{lo}=2.25$, and $W_{lo}=0.7a$, as they are typical values that could be used in experiments. In addition we have assumed $\epsilon=1$ in the region above the PhC. The gray-shaded region represents modes that can propagate in air. In order to show how the dispersion relation for the surface state changes with the thickness of the defect layer, we have also plotted in Fig. 2(a) the results for three different values of W_d (magenta, blue, and orange

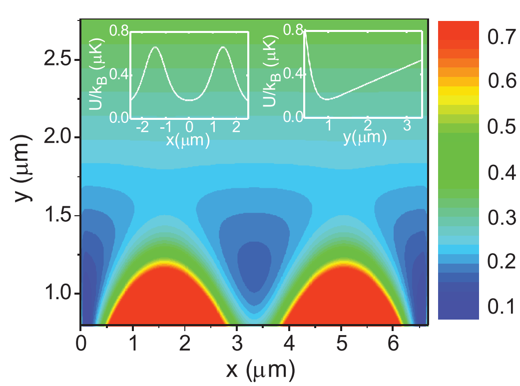

FIG. 4. (Color) 2D total atomic potential produced by the structure sketched in Fig. 1 in the xy plane for the case of Cs atoms. Color scale codes the potential in units of microkelvins. The minimum is found at $(x_0,y_0)=(3.3,1.1)$ μm. Left and right insets show cross sections of the potential along the lines $y_0=1.1$ μm and $x_0=3.3$ μm, respectively.

lines correspond to $W_d=0.04a$, $0.07a$, and $0.1a$). Any of these values for W_d could be chosen for our design; for definiteness, from now on we take $W_d=0.07a$.

Now, let us turn our attention to studying how the electric field profile depends on the frequency of the defect mode. Figure 2(b) shows a cross section in the y direction of electric field intensities of the surface states corresponding to three representative frequencies near the light line. Blue, green, and red lines show the results for $\omega a/2\pi c=0.214$, 0.225, and 0.235, respectively. The profile of the dielectric constant along the y direction of the structure has also been plotted. As is expected, the decay length in air increases as we get closer to the light line (i.e., as the frequency decreases). In addition, notice that in all three cases the electric field intensity inside the PhC decreases to almost zero over a distance of $3a$. This fast decay would allow a practical implementation of the proposed structure, consisting of just 3–4 periods of the PhC.

At this point, it is worth taking a closer look at the advantages of the type of systems studied in this work compared with other kinds of rigid dielectric structures that are not based on PhCs. As shown in Fig. 2(a), the dispersion relation of the defect mode of a PhC allows us to choose a frequency as close to the light line as we need in our atomic trap design; thereby, the decay length in air can be tuned to be arbitrarily long. However, this property could not be obtained by means of any TIR-based waveguide placed on top of a dielectric substrate, as in that case the frequencies of the confined states ω_d are such that $\omega_d < ck_{\parallel}/\sqrt{\epsilon_s}$, where ϵ_s is the dielectric constant of the substrate. This point is illustrated in Fig. 2(a), where the green-shaded area corresponds to the region where confined states can exist for the case $\epsilon_s=\epsilon_{lo}$. As we can see in that figure, all of those states are far from the light line, so their decay length in air is short.

Now, before proceeding with the analysis of the full waveguiding structure, let us examine the confining atomic potential created by the 1D PhC with a defect described previously, but without waveguides. If we illuminate this defect layer with a laser beam whose frequency ω is blue detuned with respect to a certain atomic transition of frequency ω_0, then an atom located above the PhC will experience a potential given by the sum of the optical-dipole (U_{op}), gravitational (U_{gv}), and Casimir-Polder interactions (U_{CP}), that is, $U(\mathbf{r})=U_{op}(\mathbf{r})+U_{gv}(\mathbf{r})+U_{CP}(\mathbf{r})$. The optical dipole contribution can be written as [14,18]

$$U_{op}(\mathbf{r}) = \beta_s \frac{\hbar\Gamma^2}{8\Delta}\frac{I(\mathbf{r})}{I_{sat}} \tag{1}$$

where β_s and I_{sat} are two parameters whose values depend on the atomic transition we are considering, Γ is the corresponding linewidth, and $\Delta=\omega-\omega_0$ [note that, in deriving Eq. (1), it has been assumed that $|\Delta| \ll \omega_0$]. $I(\mathbf{r})=\frac{1}{2}\epsilon_0|\mathbf{E}(\mathbf{r})|^2$ is the electric field intensity. Since we are currently assuming that our structure has translational symmetry in both the x and z directions, we can write $I(\mathbf{r})=I_0\exp(-2y/\Lambda)$, where Λ defines the evanescent decay length of the electric field and I_0 is the intensity just above the illuminated layer.

The second term in Eq. (1) represents the gravitational potential and it is given by $U_{gv}(\mathbf{r})=mgy$, where m and g stand for the mass of each atom and the gravitational acceleration, respectively. Finally, the last term of Eq. (1) corresponds to the so-called Casimir-Polder potential $U_{CP}(\mathbf{r})=-C_4/y^3$, where the constant C_4 is given by [19]

$$C_4 = \frac{3\hbar c\alpha}{32\pi^2\epsilon_0}\psi(\epsilon_{hi}). \tag{2}$$

In the above expression, α is the atomic polarizability and the value $\psi(\epsilon_{hi})=0.69$ has been computed using the analytical expressions for the function $\psi(\epsilon_{hi})$ given by Yan *et al.* [20,21].

In order to show the feasibility of the experimental realization of the system presented in this work, we consider the case of Cs atoms, since the confinement of a condensate of Cs atoms in a similar structure has been demonstrated [13]. As we are considering the D_2 resonant transition, we must take the following values in Eq. (1): $\beta_s=2/3$, $I_{sat}=1.1\ \mathrm{mW/cm^2}$, $\omega_0=2\pi\times 3.5\times 10^{14}$ Hz ($\lambda_0=857.1$ nm), and $\Gamma=2\pi\times 5.3\times 10^6$ Hz. Regarding the external illumination, we assume that it is produced by a Ti:sapphire laser at $\omega=2\pi\times 3.6\times 10^{14}$ Hz. In addition, to get an optical potential with a similar depth to that obtained in Ref. [13], we suppose that the maximum electric field intensity in the air region very close to the PhC-air interface is $I_0=2.67\times 10^6\ \mathrm{mW/cm^2}$.

Figure 3 plots the total atomic potential as a function of the distance from the surface for several values of the decay length Λ ranging from 0.1 to 0.6 μm. As shown in this figure, a decrease in Λ leads to a shift of the minimum of the potential toward the surface. However, as can be seen, there exists a minimum distance from the surface where the condensate can be trapped, since if we take $\Lambda < 0.2\ \mu$m the total potential does not have a minimum. This limit is established by the fact that in the region where the repulsive optical potential is not negligible for $\Lambda < 0.2\ \mu$m, the Casimir-Polder attractive interaction dominates, preventing the formation of a minimum in the total potential. In the case of the corresponding TIR waveguide design with a substrate with $\epsilon=2.25$ one would obtain a maximum decay length $\Lambda < 0.12\ \mu$m; thus, given the rapid variation of Casimir-Polder interaction as a function of distance, this demonstrates explicitly that a TIR scheme cannot be made to work for the current purpose, and that PhCs indeed have to be used.

Since we are interested in bringing the BEC as close as possible to the surface, we will choose $\Lambda=0.3\ \mu$m. This value corresponds to a state of wave vector $k_{\parallel}a/2\pi=0.27$ of the defect band, and thereby a value of the periodicity $a=0.19\ \mu$m [see Fig. 2(a)]. From now on, we will assume this value of $k_{\parallel}$, unless otherwise stated. In that case, the minimum of the potential appears at $y_0=1.1\ \mu$m.

It is also interesting to analyze the contribution of each term appearing in Eq. (1) to the total atomic potential. Blue, green, red, and black lines in the inset of Fig. 3 show the total, optical, gravitational, and Casimir-Polder potentials, respectively, for $\Lambda=0.3\ \mu$m. This figure reveals that at small distances the Casimir-Polder potential governs the behavior of the total potential while for distances slightly larger than y_0, the total potential is dominated by the gravitational interaction.

Now, let us focus on how to obtain a suitable confining potential in the x direction, needed to create an optical BEC waveguide. As we described above, we could solve this problem by including in the defect layer two index-guided waveguides of dielectric constant ϵ_w, with $\epsilon_w > \epsilon_{hi}$ (see schematics in Fig. 1). For definiteness, we take $\epsilon_w = 18$ [22]. The mode we explore is the even mode of this system of two coupled waveguides. In order to reproduce faithfully the features that could be found in the experiments, we have simulated the structure using the finite-difference time-domain method [23]. The results obtained with this method come from exact solutions of the 3D Maxwell equations, except for the numerical discretization.

As we described in the introduction, one of the main advantages of our proposal is that there are several parameters that can be changed at our convenience. Through the previous calculations, we have fixed the values of the thickness of the defect layer W_d, as well as the wave vector k and the frequency ω considered. In addition, now for simplicity, we fix the width of the waveguides to $W_w = 2a$. Therefore, the remaining parameters in our optimization process are the distance between the waveguides H_w and the power P_0 carried by the even mode they create. We now look for the values of (H_w, P_0) such as the curvature of the potential at its minimum is similar both in the x and the y directions. This condition would be useful if we want to guide a cylindrical-shape BEC along our waveguide. In addition, notice that we require a low value of P_0 in order to have an efficient guiding system.

Following the program described above, we have found a suitable configuration for $H_w = 3.2$ μm and $P_0 = 0.1$ mW. Figure 4 shows a contour plot of the corresponding two-dimensional total atomic potential in the xy plane. The color scale codes the potential in units of microkelvins. This figure shows a minimum at $(x_0, y_0) = (3.3, 1.1)\mu$m, being the center of the waveguides located at $x_1 = 1.5$ μm and $x_2 = 5.1$ μm. Left and right insets plot cross sections along $y_0 = 1.1$ μm and $x_0 = 3.3$ μm, respectively. From these cross sections, we find that the trap frequency at the minimum along the x axis is $\omega_x = 1233$ Hz, while along the y axis it is $\omega_y = 642$ Hz. This corresponds to a ratio $\omega_x / \omega_y = 1.92$, which confirms that it is possible to get a confining potential with similar curvatures in both transverse directions using this configuration. Notice that, with the same power, we could get other shapes for the BEC by changing the ratio ω_x / ω_y through the variation of H_w.

Finally, a few words on how to couple our system to an external source are pertinent. For this purpose, we take advantage of the well-known techniques developed to couple light with other kinds of surface states, for instance surface plasmons [24]. Thus, either a grating coupler or an attenuated total reflection device (such as a prism under total internal reflection conditions) can be considered as appropriate candidates for exciting the surface electromagnetic modes appearing in our system.

In conclusion, we have proposed a class of optical BEC waveguides based on illuminating two waveguides built into a defect of a 1D PhC. We have demonstrated that a power as low as 0.1 mW is enough to guide a BEC of Cs atoms through the suggested waveguide at about 1 μm above the structure. The kind of system proposed in this work could be considered as a basic ingredient for the development of BEC on-chip devices.

We are thankful to Wolfgang Ketterle for providing inspiration and suggestions for this work. J.B.A. acknowledges financial support by the Spanish MEC under Grant No. BES-2003-0374.

[1] A. E. Leanhardt *et al.*, Phys. Rev. Lett. **89**, 040401 (2002).
[2] D. M. Stamper-Kurn *et al.*, Phys. Rev. Lett. **80**, 2027 (1998).
[3] S. Inouye *et al.*, Nature (London) **392**, 151 (1998).
[4] M. J. Renn *et al.*, Phys. Rev. Lett. **75**, 3253 (1993).
[5] H. Ito *et al.*, Phys. Rev. Lett. **76**, 4500 (1996).
[6] J. Yin *et al.*, J. Opt. Soc. Am. B **15**, 25 (1998).
[7] A. H. Barnett *et al.*, Phys. Rev. A **61**, 023608 (2000).
[8] J. Arlt *et al.*, Phys. Rev. A **63**, 063602 (2001).
[9] J. P. Burke *et al.*, Phys. Rev. A **65**, 043411 (2002).
[10] V. I. Balykin *et al.*, Phys. Rev. A **70**, 011401(R) (2004).
[11] F. Le Kien, V. I. Balykin, and K. Hakuta, Phys. Rev. A **70**, 063403 (2004).
[12] X. Luo *et al.*, Opt. Lett. **29**, 2145 (2004).
[13] D. Rychtarik *et al.*, Phys. Rev. Lett. **92**, 173003 (2004).
[14] R. Grimm, M. Weidemuller, and Y. Ovchinnikov, Adv. At., Mol., Opt. Phys. **42**, 95 (2000).
[15] P. Yeh, A. Yariv, and C. S. Hong, J. Opt. Soc. Am. **67**, 431 (1977); A. Y. Cho, A. Yariv, and P. Yeh, Appl. Phys. Lett. **30**, 471 (1977); P. Yeh, A. Yariv, and A. Y. Cho, *ibid.* **32**, 104 (1978); J. D. Joannopoulos, R. D. Meade, and J. N. Winn, *Photonic Crystals: Molding the Flow of Light* (Princeton University Press, Princeton, NJ, 1995); F. Ramos-Mendieta and P. Halevi, Opt. Commun. **129**, 1 (1996); V. M. Robertson, J. Lightwave Technol. **17**, 2013 (1999).
[16] H. A. Haus, *Waves and Fields in Optoelectronics* (Prentice-Hall, Englewood Cliffs, NJ, 1984).
[17] S. G. Johnson and J. D. Joannopoulos, Opt. Express **8**, 173 (2001).
[18] V. I. Balykin *et al.*, Rep. Prog. Phys. **63**, 1429 (2000).
[19] Y. J. Lin *et al.*, Phys. Rev. Lett. **92**, 050404 (2004).
[20] Z. C. Yan, A. Dalgarno, and J. F. Babb, Phys. Rev. A **55**, 2882 (1997).
[21] Although the calculation of the Casimir-Polder attraction of the full multilayer structure would require a more detailed analysis, by taking only the higher dielectric constant we obtain an upper limit for the strength of this interaction.
[22] Equivalently, bearing in mind a possible experimental implementation, one could choose a smaller value of ϵ_w and a larger local thickness $W_d(x)$, of the defect layer.
[23] A. Taflove and S. C. Hagness, *Computational Electrodynamics: The Finite-Difference Time-Domain Method*, 2nd ed. (Artech, Norwood, MA, 2000).
[24] H. Raether, *Surface Plasmons* (Springer-Verlag, Berlin, 1988).